Angular Scattering Analysis of the Circular Dichroism of Biological Cells. 1. The Red Blood Cell Membrane†

Adina Gitter-Amir,‡ Kurt Rosenheck,* and Allan S. Schneider§

ABSTRACT: A quantitative interpretation of the distorted circular dichroism spectrum of red blood cell membranes is presented including the effects of the intense small angle scattering and light detection geometry of our spectrophotometers. Corrected spectra have been obtained by nondestructive methods which correspond to an in situ membrane protein conformation of 45% α helix, 10% β sheet, and a conformational precision of better than ±10%. Forward scattering calculations which neglect the small angle scattering collected by conventional phototube acceptance angles are shown to be unsuitable for red cell membranes. Ultraviolet refractive index dispersion has been estimated for the membranes together with an evaluation of the sensitivity of the calculated spectrum to this variable. Angular scattering and circular dichroism calculations are extended to two alternative models for the location of hemoglobin in "pink ghosts", and it is indicated that this approach might help in resolving the question whether residual hemoglobin is in solution inside the ghost, or is part of its membrane.

During the last few years much progress has been made in extending ultraviolet optical activity and absorption spectroscopy to turbid suspensions of complex biological particles. The work thus far has focused on separating turbidity effects (scattering and absorption flattening) from the intrinsic molecular spectra, and using the latter to derive structural information for the macromolecules in situ in the biological system. Both calculational and experimental methods have been used; the former for suspensions of biological membranes (Gordon and Holzwarth, 1971; Gordon, 1972; Rosenheck and Schneider, 1973; Urry, 1972), polypeptide aggregates (Gordon, 1972), subcellular secretory vesicles (Rosenheck and Schneider, 1973), and viruses (Holzwarth et al., 1974), and the latter for membranes (Schneider et al., 1970; Glaser and Singer, 1971; Litman, 1972; Ji and Urry, 1969), viruses (Dorman and Maestre, 1973), and chloroplasts (Philipson and Sauer, 1973; Gregory and Raps, 1974). In certain cases (Rosenheck and Schneider, 1973) excellent quantitative resolution of the spectra has been obtained together with corresponding protein structural information. We believe it may now be possible to interpret the ultraviolet spectra of simple biological cells and it is this problem which forms the subject of this and the succeeding paper.

In the present work we perform a calculational interpretation of the ultraviolet absorption and circular dichroism (CD)[1] spectra of the human red blood cell (RBC). Such spectra contain essential information on the cell's protein secondary structure, composition, and morphology. We chose the red blood cell since it is among the simplest and best-defined of cells, contains primarily one protein of known structure (hemoglobin), and, thus, has the built-in controls with which to test the calculational analysis. The special problems which arise in interpreting the spectra of the red cell are characteristic of large (relative to wavelength), absorbing, scattering particles and will be common to other more complex biological cells. As such, the present analysis of red cell spectra can serve as a prototype for interpretation of the CD and absorption spectra of other cellular systems.

An important aspect of the present analysis, which is particularly relevant to large size particles (e.g., biological cells) and has not been previously treated, is our calculation of the angular dependence of circular dichroism. Most previous calculations (Gordon and Holzwarth, 1971; Gordon, 1972; Rosenheck and Schneider, 1973; Holzwarth et al., 1974) of scattering contributions to optical activity spectra have considered only the forward direction, thus, counting all light scattered at non-zero angles as an extinction. Large size particles, however, are known to have an intense small angle scattering which for conventional spectrophotometers may not be excluded by the acceptance angle of the phototube. Thus, a discrepancy can exist between the forward scattering calculation which excludes all non-zero angles in the transmitted beam and spectroscopic measurements with conventional instrumentation that may not exclude the intense small angle scattering. We indeed demonstrate in this and the succeeding paper that for cell size particles in the uv region of the spectrum it is important to calculate the angular scattering contribution to absorption and circular dichroism spectra and, thus, take into account the detector geometry of the spectroscopic instrumentation being used. These calculations will also be relevant to measurements made with recently modified instrumentation (Dorman et al., 1973) capable of large variation of its detector geometry. The angular scattering contribution to the visible absorption spectra of biological cells, has been studied before (Latimer and Eubanks, 1962; Latimer, 1972; Latimer and Pyle, 1972; Cross and Latimer, 1972). The results of their studies on absorption spectra were, however, not taken into account in studies of optical activity spectra until now.

Another interesting and potentially important aspect of angular optical activity calculations is that they may reveal

† From the Laboratory of Membranes and Bioregulation, The Weizmann Institute of Science, Rehovot, Israel (A.G.A., K.R.), and the Sloan-Kettering Institute for Cancer Research and Cornell University Graduate School of Medical Science, New York, New York 10021 (A.S.) *Received August 19, 1975.*

‡ This work derives in part from Adina Gitter-Amir's Ph.D. thesis (1974), carried out at the Feinberg Graduate School of the Weizmann Institute of Science, Rehovot, under the supervision of Dr. Kurt Rosenheck.

§ Supported by National Institutes of Health Grants CA 08748 and CA 16889.

[1] Abbreviations used are: uv, ultraviolet; CD, circular dichroism; ORD, optical rotatory dispersion; RCM, red cell membrane; RBC, red blood cell; Hb, hemoglobin; Hb/M, hemoglobin to membrane protein ratio (w/w).

information on supramolecular asymmetry and long range order, as has been observed for cholesteric liquid crystals (DeVries, 1951) and speculated on for DNA packing in viruses (Holzwarth et al., 1974; Dorman and Maestre, 1973) and membrane stacking in chloroplasts (Philipson and Sauer, 1973).

In the first part of this work we consider the red cell membrane; in the second part, we use the obtained membrane optical properties in the scattering calculation of the intact erythrocyte spectra. We use the previously described (Rosenheck and Schneider, 1973) coated-sphere scattering model for the red blood cell, with the coat representing the membrane, and the core representing the concentrated hemoglobin solution inside.

There have been several previous studies of the CD spectra and protein conformation of the red cell membrane. In general, previous efforts to reduce turbidity artifacts in the spectra have used mechanical fragmentation methods, such as sonication (Schneider et al., 1970) and French press (Glaser and Singer, 1971), or detergent solubilization (Gordon and Holzwarth, 1971). It is desirable, wherever possible, to use nondestructive methods for obtaining the corrected intrinsic spectrum, in order to avoid the possibility of small protein structural changes accompanying fragmentation or solubilization. The present analysis avoids this problem by using an iterative calculational procedure (Schneider, 1973) with various protein secondary structures and their corresponding intrinsic CD and ORD spectra (Chen et al., 1972). A scattering calculation of the turbid suspension spectrum is made and compared with the experimental suspension spectrum. The trial intrinsic spectrum which yields a good fit of calculated and experimental turbid suspension spectra is chosen as the corrected spectrum, from which the in situ protein conformation is determined. It is noteworthy that most previous estimates of membrane protein secondary structure were based on polypeptide reference spectra of limited applicability to proteins. In the present work we use the more relevant CD and ORD reference spectra derived by Chen et al. (1972) from proteins having known x-ray structures (Rosenkranz, 1974; Rosenkranz and Scholtan, 1971).

In addition to determining the secondary structure of membrane protein for white ghosts (Hb/membrane protein < 0.03) we also consider the question of whether the residual hemoglobin of pink ghosts (Hb/membrane protein ~ 2) is a part of the membrane or simply in solution within the ghost. Specifically, we calculate both CD spectra and the angular dependence of the scattering cross section for two models representing the two cases above and see whether the calculated optical properties can distinguish between them.

Experimental Methods

Human outdated blood, type O, Rh positive, was obtained from the blood bank of Kaplan Hospital, Rehovot, and used in all experiments. Red cell membranes were prepared by a procedure of gradual successive hemolysis in progressively lower hypotonic buffer, as previously described (Schneider et al., 1970). Either phosphate or Tris-HCl buffers, pH 7.4, were used as indicated in the text. The red button at the bottom of the pellet during the last washes was discarded and the final ghosts appeared milky white.

Membrane protein concentration was determined by the method of Lowry et al. (1951) with bovine serum albumin as standard.

Absorption spectra were measured on a Cary 15 absorption spectrophotometer. The acceptance half-angle, ϕ, of the Cary 15 light detection system is $8 \pm 2°$ from the center of a 1-mm path cuvette, the $\pm 2°$ depending on which part of the beam in the sample space the angle is measured from.

Circular dichroism measurements were made on a Cary 60 spectropolarimeter with 6002 CD attachment in 1-mm path cells. The acceptance half-angle, ϕ, for the CD measurement is $8.5 \pm 1.2°$ for a 1-mm path cuvette.

Calculational Methods. The general calculational approach used here for interpreting the distorted absorption and circular dichroism spectra of a turbid biological suspension has been previously described in detail (Schneider, 1973), including illustrative numerical computations for subcellular secretory vesicles (Rosenheck and Schneider, 1973), erythrocyte ghosts (Gordon and Holzwarth, 1971), and viruses (Holzwarth et al., 1974). In brief, the approach is to calculate the turbid suspension CD spectrum, including scattering and absorptive contributions, using a set of assumed trial intrinsic CD and ORD spectra corresponding to a set of protein conformations (Chen et al., 1972). The extinction is first calculated for left and right circularly polarized light separately, using the appropriate scattering functions as defined by the size, shape, and optical properties of the scattering particle. The difference in left and right extinctions is then taken as the calculated suspension CD. The overall calculation is repeated with various trial intrinsic CD and ORD spectra until a fit of calculated and experimental turbid suspension spectra is achieved.

The trial intrinsic optical activity spectra that yield the best fitting calculated suspension CD spectrum are taken as the corrected spectra (free of turbidity effects) that define the in situ protein conformation in the intact cell membrane or cell's cytoplasm.

The general form of the equation used in calculating suspension CD is:

$$CD_{susp} = -Im \frac{\pi}{\lambda} [F(m_{lp}) - F(m_{rp})] \qquad (1)$$

where Im refers to the imaginary part of a complex function, λ is wavelength, m_{lp} and m_{rp} are the intrinsic complex relative refractive indices of the particle for left and right circularly polarized light, respectively, and the function $F(m_p)$ contains the specific particle scattering function and its relation to the optical properties of a suspension of N such particles. The latter function may have a logarithmic form similar to that derived by Duysens (1956) and Amesz et al. (1961) for cases where the condition of single scattering (and absorption) in the forward direction is not observed, i.e., cases where not all particles see the initial incident light intensity. For cases of single scattering (and absorption), and where the relative, refractive index is close to one (van de Hulst, 1957) the logarithmic form can be expanded to a linear form. The assumption of independent scattering is implicit in our calculations. The intrinsic optical activity characterizing the in situ protein conformation enters the calculation via the former's relation to the complex relative refractive indices of the particle for left and right circular polarizations, m_{lp} and m_{rp}.

In the present work we extend the previously used methods outlined above to include the effects of various finite detector acceptance angles that are known to be important for scattering particles of a size comparable to and greater than the wavelength, due to their intense small-angle scattering. We use the method described by Gumprecht and Sliepcevich (1953) to calculate extinction and scattering cross sections for finite detector acceptance angles. We calculate the scattering efficiency, $Q_S(\phi)$, of the particle (membrane or intact cell) as measured by a phototube having a finite acceptance half-angle,

ϕ, around the forward direction. The absorption efficiency, Q_A, is added to $Q_S(\phi)$ to obtain the total extinction efficiency, $Q_E(\phi)$, of the particle for a given light detection geometry, defined by ϕ. The scattering, absorption, and extinction efficiencies are simply the respective normalized cross sections, and are used to calculate the CD for a suspension of particles via eq 1. The CD calculated from the total extinction efficiency, for a half-acceptance angle ϕ, is denoted by $[\theta_T]_\phi$. The CD calculated from the scattering or absorptive efficiencies is denoted by $[\theta_S]_\phi$ and $[\theta_A]$, respectively. The value of $\phi = 8°$ was used in our calculations, which are compared with measurements, since the extinction and CD spectra for $8.5 \pm 1.2°$ and $8 \pm 2°$ are practically the same. The maximum acceptance half-angle of the measurements will be $\sim 10°$, which is reasonably close to the calculated scattered ray at 8° which after refractive bending would exit the cuvette at 10–11°.

Scattering Model. We use an extension of the Mie equations for the coated sphere scattering model to simulate the sphered red cell and its membrane (Aden and Kerker, 1951). The model is illustrated in Figure 1, where r is the inner radius, Δ the membrane thickness, and m_1 and m_2 the complex refractive indices of the core and shell material, respectively, relative to that of the medium m_3. When the core and medium refractive index are equal, i.e., $m_1 = 1$, we have the hollow shell model that we use for the red cell ghost.

The specific parameters that define the scattering model (hollow shell) for the sphered red cell membrane are given below. The radius, $r = 3.26$ μm was chosen as the most probable radius for sphered ghosts (Roth and Seeman, 1972). About 85% of ghosts have $3.0 < r < 3.5$ μm; about 65% have $3.18 < r < 3.33$ μm. The membrane thickness, Δ, is taken as the generally accepted value of 10 nm. The imaginary part of refractive index, n_2', is linearly related to absorbance (van de Hulst, 1957) and was determined from the measured absorption spectrum of solubilized ghosts. Our values are similar to values obtained by Gordon and Holzwarth (1971) using sodium dodecyl sulfate solubilization. The real part of the refractive index for the RCM was determined as follows: the dependence of $Q_E(\phi)$ on n_2 was calculated for a wide range of refractive index values, for each wavelength. From these $Q_E(\phi)$ values, optical densities were calculated for an RCM suspension. These OD values were compared with the experimental OD measured with the same ϕ value on the Cary 15 spectrophotometer. The values of n_2 for which OD_{exp} was equal to OD_{calcd} were taken as the respective membrane refractive index values. The resulting relative refractive indices for the membrane in the uv were: for $\lambda = 192.5$–207.5 nm, $n_2 = 1.18$; for $\lambda = 210$–220, $n_2 = 1.16$; for $\lambda = 222.5$–235, $n_2 = 1.14$; for $\lambda = 235.5$–240, $n_2 = 1.12$. These refractive indices correspond to a protein concentration of 0.53 g/ml in a membrane with $\Delta = 10$ nm and $r_{inside} = 3.26$ μm. The trial values of the intrinsic membrane CD and ORD were chosen by assuming a given protein secondary structure and determining the corresponding CD and ORD from the protein reference spectra of Chen et al. (1972).

Calculations for "pink ghosts" (Hb/membrane protein ~ 2) were carried out for two alternative models aimed at simulating different locations of the residual hemoglobin in the ghost. One model, which we refer to as the RCM model, is the same as the hollow shell described above for the white ghosts except that the hemoglobin is a part of the membrane forming a thicker shell. The shell parameters are a mixture of Hb and membrane in proportion to the Hb/M ratio. A shell thickness of 20 nm is taken and the known optical properties of hemoglobin are used in calculating the shell parameters. The "pink ghost" RCM model, thus, treats the residual Hb as though it were a true membrane protein, irrespective of its precise location within or on the membrane, the same way that the model makes no distinction between the integral and peripheral proteins of the ghost membrane. The altogether different model in which Hb is concentrated on the inner or outer surface of the membrane, forming a separate layer, was not investigated in these calculations. The alternative model for the pink ghosts is the coated sphere, with the residual hemoglobin in solution forming the core, and the membrane the shell. We refer to this as the RBC model and the shell parameters are as described for the white ghost, while the core parameters are simply those of a hemoglobin solution of the appropriate concentration. The Hb solution parameters are specified fully in Part 2.

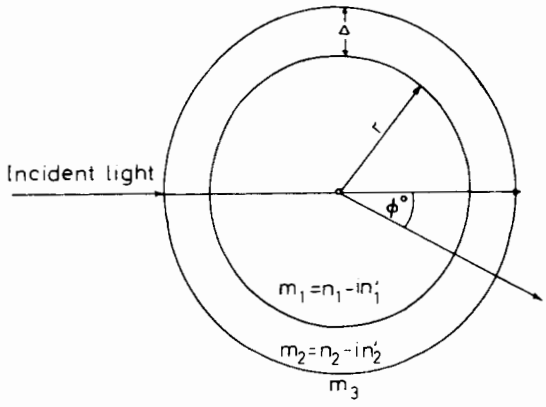

FIGURE 1: Concentric sphere scattering model with relevant parameters.

The scattering functions for the coated sphere model are an extension of the Mie equations derived by Aden and Kerker (1951) and previously applied to subcellular secretory vesicles by Rosenheck and Schneider (1973). We use the computational scheme of Pilat (1967) and Fenn and Oser (1965) in computing the extinction and scattering efficiencies in the forward direction. This computational scheme was extended to calculations of the scattering and extinction efficiencies $Q_S(\phi)$ and $Q_E(\phi)$, for detectors with finite acceptance half-angles, ϕ, according to the method of Gumprecht and Sliepcevich (1953). According to the latter, the intensity of light scattered is integrated over the angle ϕ around the forward direction and subtracted from the total scattering over all directions. The intervals used in the integration are 0.1° for 0–10°. The relatively small interval of 0.1° is used due to the steep dependence of $Q_S(\phi)$ on ϕ near the forward direction. For $\phi > 10°$, intervals of 0.2–0.4° are used. Several important computational subtleties that arise in scattering efficiency calculations for large absorbing spheres, such as the sphered red blood cell, are discussed in the Appendix, of the following paper in this issue (Gitter-Amir et al., 1976), together with the computational checks used to test our computer programs.

Results

We present below the calculated circular dichroism spectra for turbid suspensions of red cell membranes. The sensitivity of the calculated spectra to detector acceptance angle and trial protein conformation is first shown (Figures 2–4). This is followed by a comparison of calculated and experimental suspension spectra for the best fitting conformation, together with a resolution of the distorted membrane spectrum into scattering and absorptive contributions (Figure 5). In addition, we contrast calculated suspension optical properties for two

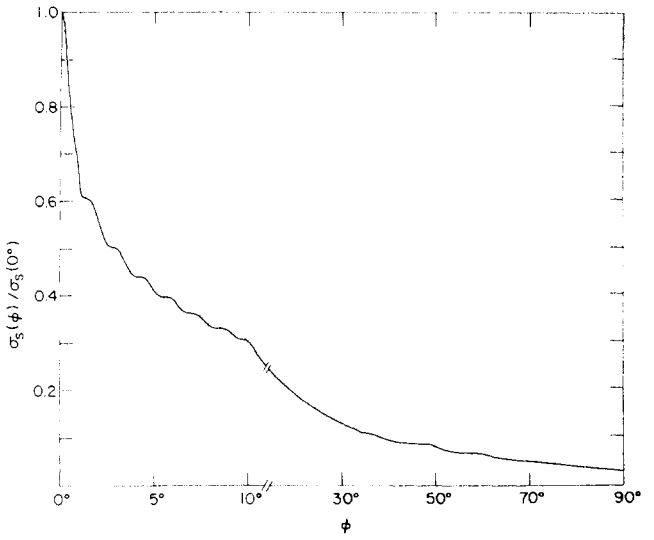

FIGURE 2: Dependence of the calculated relative scattering cross section, $\sigma_S(\phi)/\sigma_S(0°)$, for RCM particles, on detector acceptance half-angle ϕ. λ 225 nm; $m_2 = 1.14 - 0.016i$.

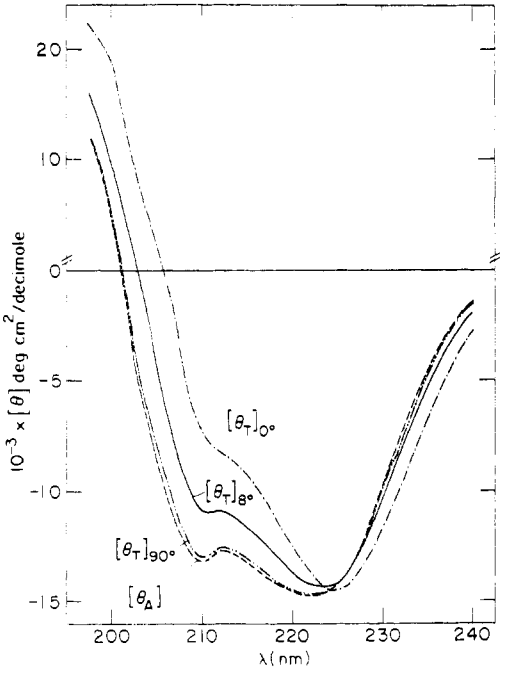

FIGURE 3: Dependence of calculated CD spectra of RCM suspension on detector acceptance half-angles. Intrinsic protein conformation: $\alpha = 45\%$; $\beta = 10\%$; rest unordered. (- · · · -) $(\theta_T)_{0°}$; (—) $(\theta_T)_{8°}$; (- · · · · · -) $(\theta_T)_{90°}$; (- - - - -) (θ_A).

alternative models representing the location of residual hemoglobin in pink ghosts (Figures 6, 7).

Figure 2 shows the dependence of the relative scattering cross section on detector acceptance half-angle, ϕ, at a wavelength of 225 nm (near the CD trough). The relative scattering cross section, $\sigma_S(\phi)/\sigma_S(0°)$, represents the fraction of total scattered light, $\sigma_S(0°)$, excluded from a detector with acceptance half-angle ϕ. Since there is only a weak dependence on n_2 and on λ, it is sufficient to show one representative curve for RCM. It can be seen that a significant portion of the total scattering lies within relatively small angles near the forward direction. Consequently, a conventional absorption spectrophotometer with acceptance half-angle of about 10°, e.g. Cary 15, will only detect about 30% of the scattered light as an extinction. By increasing the solid angle of detection to about 90° Figure 2 would predict that now only 3% of the scattering would be excluded from the phototube.

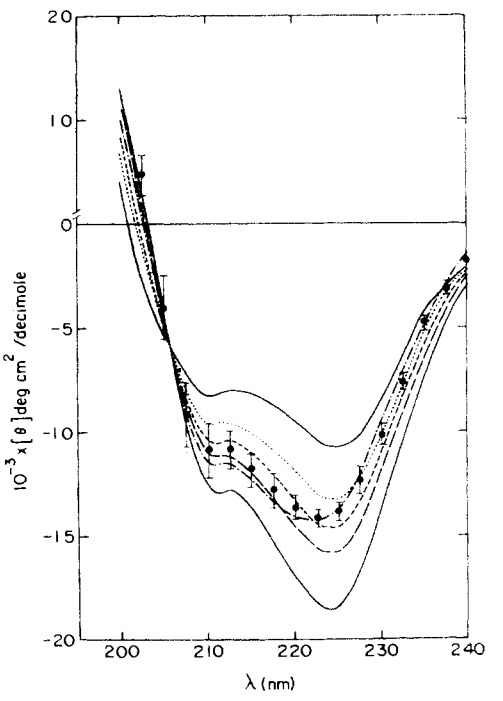

FIGURE 4: Dependence of calculated CD spectra ($\phi = 8°$) of RCM suspension on trial intrinsic protein conformation. The experimental suspension CD is shown by the fitted circles. The error bars represent the reproducibility of various measurements of different RCM suspensions prepared in phosphate buffer. Upper (—) $\alpha = 30\%$, $\beta = 0\%$; (· · · ·) $\alpha = 40\%$, $\beta = 0\%$; (- - - -) $\alpha = 45\%$, $\beta = 0\%$; (- · · · · ·) $\alpha = 45\%$, $\beta = 20\%$; (- - -) $\alpha = 50\%$, $\beta = 0°$; lower (—) $\alpha = 60\%$, $\beta = 0\%$.

In Figure 3 we show the effect of acceptance angle on calculated membrane CD spectra for an intrinsic conformation of 45% α helix and 10% β structures. It is interesting to note the difference between the forward scattering calculation (0° acceptance half-angle) and 8° acceptance half-angle that corresponds to the Cary 6002 circular dichrometer. The main effect is seen to be at the 210-nm trough which is more distorted for the forward scattering case. As will be seen in Figure 5 below, the 8° calculation gives a good shape and magnitude fit to experimental spectra measured at similar acceptance half-angle, ϕ. For ϕ equal to 90° the membrane CD spectrum is seen to closely resemble the absorptive part of the spectrum, $[\theta_A]$, which means that the differential scattering contribution at $\phi = 90°$ to the overall CD is very small. At 90°, indeed, as seen from Figure 2, most of the scattered light is collected.

In Figure 4 we present the conformational sensitivity of the calculated membrane CD spectra. It is important to demonstrate such sensitivity before drawing conclusions about protein structure, since the calculated spectra must be able to distinguish between various trial protein conformations in order to be sure that the determined protein structure is unique. Figure 4 indicates that a change of 10% helix in trial protein structure will result in an increment of 2500 units of molar ellipticity (deg-cm^2/dmol) at the 225-nm trough. A slightly lower sensitivity to β-sheet structure is shown in Figure 4. It should thus be possible to distinguish membrane protein secondary structures within 10% or better.

Figure 5 compares the experimental membrane suspension spectrum with the best fitting calculated suspension CD spectrum. The corrected intrinsic spectrum used for the best-fit

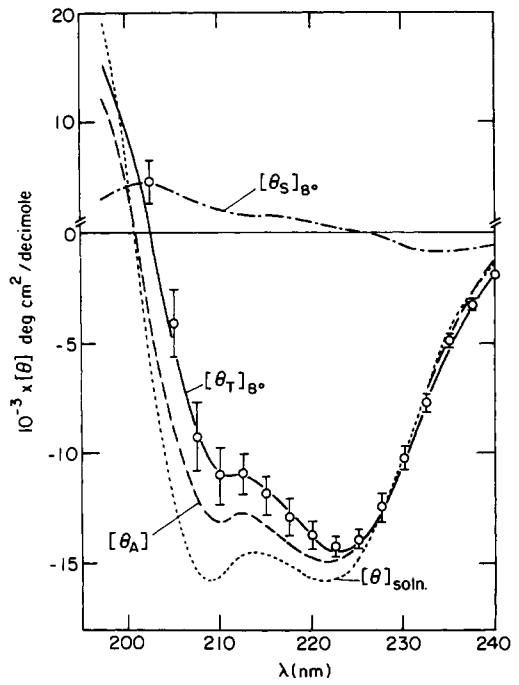

FIGURE 5: Experimental CD spectrum of RCM suspension and best fitting calculated $\phi = 8°$ spectrum. Experimental points, same as in Figure 4. (—) Calculated suspension spectrum for intrinsic protein conformation, $\alpha = 45\%$, $\beta = 10\%$, rest unordered; (· · · · ·) calculated solution CD for a protein of $\alpha = 45\%$, $\beta = 10\%$, rest unordered; (- - - -) calculated absorptive contribution; (- · · · -) calculated differential scattering contribution for $\phi = 8°$.

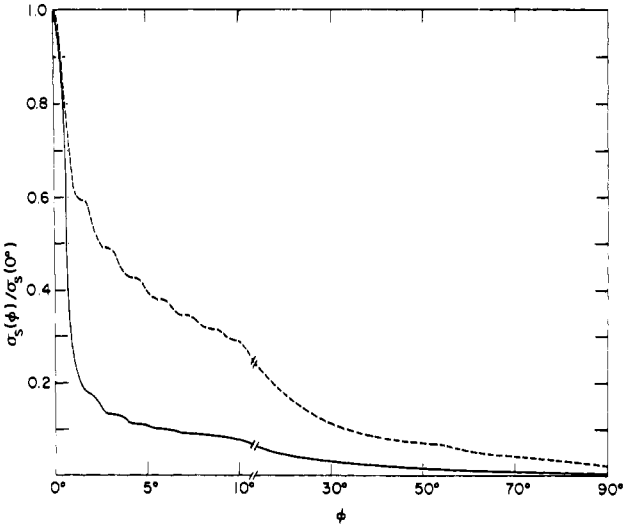

FIGURE 6: Dependence of the calculated relative scattering cross section, $\sigma_s(\phi)/\sigma_s(0°)$, on detector acceptance half-angle ϕ, for pink ghost particles of Hb/M = 2. $\lambda = 225$ nm. (- - -) RCM model; (—) RBC model. For the RCM model: $\Delta = 20$ nm; $m_2 = 1.14 - 0.0163i$. For the RBC model: $\Delta = 10$ nm, $m_2 = 1.14 - 0.016i$, $m_1 = 1.001818 - 0.0003i$.

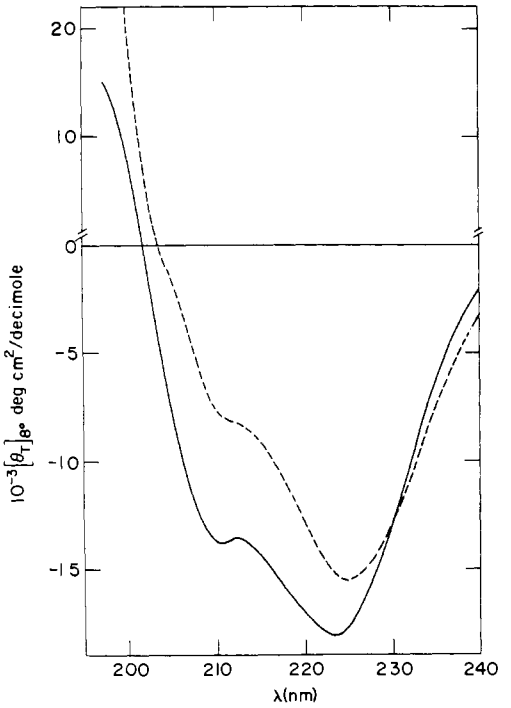

FIGURE 7: Calculated CD spectra for a suspension of pink ghosts of Hb/M = 2. $\phi = 8°$. The parameters are specified in the computational model section in the text. (- - -) RCM model; (—) RBC model.

calculation is shown and corresponds to an in situ membrane protein structure of 45% α helix, and 10% β sheet. The fit is seen to be quite good, and the determined average protein structure should, thus, be as good an estimate for the red cell membrane as can currently be made. A breakdown of the calculated turbid membrane suspension CD into differential scattering and absorptive contributions is also shown. The distorting loss of CD intensity near 208 nm is seen to result about equally from differential scatter and absorption flattening, while the red shift in crossover wavelength is seen to come from the differential scatter alone. The shape of the differential scatter has a striking resemblance to an α helical ORD curve as previously predicted (Schneider, 1971, 1973; Gordon, 1972).

Figures 6 and 7 represent calculated optical properties for different models of hemoglobin location within pink ghosts for a hemoglobin to membrane protein ratio of 2. In one model, which we call the RCM model, the residual hemoglobin of the pink ghost is part of the membrane. In the second model, the RBC model, the hemoglobin is in solution within the ghost. The plots of relative scattering cross section, $\sigma_S(\phi)/\sigma_{S(0°)}$ vs. acceptance half-angle, ϕ, in Figure 6 are seen to be different for the two models, with the RBC model showing a greater percentage of the total scattered light being concentrated near the forward direction. For example, the RBC has about 70% of its scattered light concentrated within an acceptance half-angle of 1°, while the RCM model has only 40% within this angle.

It may be possible to distinguish between the alternative locations of the hemoglobin in pink ghosts by calculated CD spectra for the two models. Figure 7 indicates a greater distortion (loss of 210 nm CD intensity relative to 225 nm) for the RCM model than for the RBC model. It will be interesting to compare future experimental scattering and CD measurements for such pink ghosts (Hb/membrane protein ~ 2) with the above calculated properties.

Discussion

We have provided a quantitative interpretation of the distorted circular dichroism spectrum of red blood cell membranes, taking into account the intense small angle scattering and the light detection geometry of our spectrophotometers. Corrected spectra have been obtained which correspond to an in situ membrane protein conformation of 45% α helix, 10% β sheet, and 45% random coil, and a conformational precision of better than ±10%. In addition, an estimate of ultraviolet refractive index dispersion was obtained for the membranes using a procedure of fitting calculated and experimental ab-

sorption spectra with trial refractive index values. We were able to completely account for the difference between a turbid membrane CD spectrum and the equivalent molecularly dispersed protein solution spectrum on the basis of differential scatter and absorption flattening, without having to invoke long-range order or speculations on supramolecular asymmetry.

The values we obtained for membrane protein conformation compare favorably with previous estimates of 40–50% α helix based on CD spectra that were experimentally corrected for turbidity by mechanical fragmentation (Schneider et al., 1970; Glaser and Singer, 1971; Litman, 1972) and detergent solubilization (Gordon and Holzwarth, 1971). In the present analysis, however, the use of nondestructive methods and protein reference spectra avoid uncertainties about sonication, French press, and detergent solubilization effects on protein structure, and questions about the limited applicability of polypeptide reference spectra to membrane proteins. Our values of membrane ultraviolet refractive index are also in good agreement with the previous estimates of Urry et al. (1971), Rosenheck and Schneider (1973), and Holzwarth et al. (1974) for mitochondria, chromaffin granule membranes, and viral coats, respectively.

During the course of this analysis we have shown how the uv absorption and CD spectra of a suspension of red cell membranes depend on the geometry of the light detection system, on the one hand, and on the intrinsic optical properties of the particle, on the other. This represents the first detailed evaluation of the effect of detector acceptance angle on the calculated CD spectrum of a turbid biological suspension. For particles the size of red cell membranes a forward scattering calculation that assumes a zero acceptance angle (Gordon and Holzwarth, 1971) will be unsuitable for simulating experimental spectra measured with the usual 8° acceptance half-angle, as was seen in Figures 2 and 3. Further discussion of this point is given in the succeeding paper, Part 2, where the fraction of light collected by the conventional 8° detection geometry is presented for a wide range of particle sizes for both hollow shell and coated sphere scattering models.

Other workers have noted the importance of small angle scattering and light detection geometry on turbid suspension CD spectra, and most previous attempts to account for it have been experimental. Thus, Dorman et al. (1973) have designed a modification of the Cary 6001 CD spectropolarimeter and also a fluorescent jacketed optical cuvette aimed at increasing the effective light acceptance angle up to 135°. However, their minimum acceptance half-angle ϕ is 11° which already collects most of the scattered light of cell size particles. Using a similar approach, Philipson and Sauer (1973) have reported dramatic effects on the CD spectra of intact chloroplasts upon changing the acceptance half-angle from 2.3 to 85°. Gregory and Raps (1974) have also examined the CD spectra of chloroplasts using a more elaborate modification of their circular dichrometer designed not only to measure the small angle differential scatter but also larger angle CD effects. They confirm the large fraction of light scattered at small angles and use a semiempirical calculation to correct their spectra. Their interpretation of the differential scatter for chloroplasts is different from that proposed by Philipson and Sauer (1973).

Using a semiempirical approach to the CD scattering question Urry (1972) built a special OD measuring accessory to his CD instrument, so that OD and CD are both measured with the same acceptance angle. The need for such an accessory will depend on the particular system studied. For RCM suspensions the normal acceptance angles of the Cary 60 spectropolarimeter and Cary 15 spectrophotometer collect practically the same amount of scattered light and so such an accessory is unnecessary for this system. Gordon and Holzwarth (1971) neglected the small angle scattering in their calculational analysis of RCM CD spectra. They assumed at the outset that "the solid angle of scattered light intercepted by the detector is sufficiently small that light scattered at non-zero angles may be neglected". They based this assumption on a lack of observable change in OD and CD spectra upon reduction of the acceptance angle with an iris diaphragm. Our calculations (Figure 2) indicate that most of the scattered light is confined to a cone defined by $\phi < 3°$ and that it may be possible to reduce the detector acceptance half-angle from 8° to 3° with relatively little change in the spectra. Thus, their observation of no change in the spectra with an undefined reduction in acceptance angle does not validate their assumption. Furthermore, the use of a single diaphragm in front of the collecting lens, no matter how small the aperture, would still permit light scattered at angles of 2–4° to reach the phototube due to the height of the beam in the sample space. Wallach et al. (1973) have performed Mie scattering calculations similar to Gordon and Holzwarth (1971) for turbid membrane suspensions, only using polylysine optical properties rather than those of solubilized membrane proteins to define their hollow shell model. They were not able to simulate the turbid membrane CD spectrum below 215 nm and reach the conclusion that "light scattering does not adequately account for the optical activity of membranes containing appreciable proportions of nonhelical conformation". These authors correctly point out the inaccuracy of synthetic polypeptide reference spectra for application to proteins. However, it is this very fact that invalidates their conclusions. If synthetic polypeptide reference spectra are invalid for application to proteins, then there is no reason to expect Mie scattering contributions to polylysine shell spectra to simulate experimental turbid membrane protein spectra. Furthermore, these authors also neglect the effects of detector acceptance angle and use a forward scattering calculation ($\phi = 0°$), which we have demonstrated in Figure 3 to be inappropriate for simulating membrane CD measured with acceptance half-angles of about 8°. Glaser and Singer (1971) (Appendix A, with Zimm) in early calculations of suspension CD mention the fact that for red cell membranes the fraction of light scattered near the forward direction can be very large and consider this in their derivation. However, they do not present calculations of the angular dependence of the scattering.

Our estimate of membrane refractive index dispersion, $n_2(\lambda)$, will have a small uncertainty that will carry over into the determination of membrane protein conformation. For a protein conformation of 45% α helix and 10% β sheet, the maximal error introduced in the calculated membrane CD at 210 nm would correspond to $\pm 5\%$ α helix and $\pm 10\%$ β sheet for acceptance half-angles greater than 3°. Wavelengths longer than 210 nm are less sensitive to refractive index. It should be noted that CD spectra calculated for the forward direction, $\phi = 0°$, have a greater refractive index sensitivity and, therefore, uncertainty due to refractive index error. For RCM suspensions our calculations indicate that wavelengths greater than 225 nm have a relatively low CD sensitivity to refractive index, n_2. Therefore, at these wavelengths an exact knowledge of membrane refractive index is not required. It is useful to note that a change in α helix would cause CD changes in the same direction at 210 and 235 nm, while a change in refractive index will cause changes in opposite directions at these wavelengths for red cell membranes.

In previous studies of RCM structure and function different methods of ghost preparation were used which in turn resulted in membranes having different residual hemoglobin contents (Bramley and Coleman, 1972; Hanahan, 1973; Schwoch and Passow, 1973). Furthermore, it is of interest to know whether or not hemoglobin is an integral plasma membrane protein of the erythrocyte. Our calculated angular scattering pattern (Figure 6) and CD spectra (Figure 7) for two alternative models of hemoglobin within "pink ghosts" are sufficiently different to be experimentally distinguished. It should thus be possible to locate hemoglobin in pink ghosts in future angular scattering and CD measurements.

After this work was completed, Bohren (1974, 1975a,b) reported a formal derivation of circularly polarized scattering by optically active spheres and shells, in which a rigorous solution of Maxwell's equations was claimed, and angular CD scattering effects were calculated (1975a). Bohren's solution results in a scattering amplitude matrix having different elements from that used by us and by Gordon and Holzwarth (1971), and Gordon (1972). Both we and Gordon and Holzwarth have approximated the forward scattering matrix for optically active particles (in the linear basis) by assuming (a) the diagonal elements are the same as the nonoptically active particle, e.g., the Mie functions, and (b) the off-diagonal elements are the difference between diagonal elements calculated separately for left and right circular refractive indices (Schneider, 1971). Since optical activity is represented by the off-diagonal elements of the forward amplitude matrix (in the linear basis), this approximation is equivalent to a calculation of differential scatter by simply performing separate Mie computations for left and right circular refractive indices and subtracting one from the other to obtain the scattering circular dichroism. This is exactly what we have done.

Upon comparing this approximation with Bohren's expression for optical activity in terms of the explicit scattering coefficients with left and right circular refractive indices, no obvious insight into the nature of our approximation with respect to electromagnetic theory results. However, there are several important points to be made concerning the approximation that we use. First, in the limit of the nonoptically active particle, $m_{lp} = m_{rp}$, our forward scattering matrix reduces to the correct nonoptically active matrix. Secondly, our forward scattering matrix has the correct symmetry properties defined by van de Hulst (1957) for the optically active particle (Schneider, 1971; Bohren, 1975). Thirdly, and most important, Bohren (1975a) has compared numerical computations of optical activity for large scattering particles (polyglutamic acid spheres) using both our approximate theory and the exact theory. His calculations are for spheres up to 2.0 μm in diameter and a relative refractive index up to 1.49 in the far-ultraviolet region (240–190 nm). Excellent agreement was achieved between the two theories, the maximum differences being 5–10% (Bohren, 1975a). The relative refractive indices that we use for membranes in the uv are less than 1.2. For hemoglobin inside the sphered erythrocyte, the relative refractive index is lower (1.05). One might expect even closer agreement between the two theories for these more realistic lower relative refractive indices.

Acknowledgments

We thank Miss A. Zakaria and Mrs. B. Romano for their skillful technical assistance and Mrs. Y. Sheraga for valuable assistance with the computer programming.

References

Aden, A. L., and Kerker, M. (1951), *J. Appl. Phys. 22,* 1242.
Amesz, J., Duysens, L. N. M., and Brandt, D. C. (1961), *J. Theor. Biol. 1,* 59.
Bohren, C. F. (1974), *Chem. Phys. Lett. 29,* 458.
Bohren, C. F. (1975a), Ph.D. Thesis, Dept. of Physics, University of Arizona.
Bohren, C. F. (1975b), *J. Chem. Phys. 62,* 1566.
Bramley, T. A., and Coleman, R. (1972), *Biochim. Biophys. Acta 290,* 219.
Chen, Y. N., Yang, J. T., and Martinez, H. M. (1972), *Biochemistry 11,* 4120.
Cross, D. A., and Latimer, P. (1972), *Appl. Opt. 11,* 1225.
De Vries, H. (1951), *Acta Crystallogr. 4,* 219.
Dorman, B. P., Hearst, J. E., and Maestre, M. F. (1973), *Methods Enzymol. 27D,* 767.
Dorman, B. P., and Maestre, M. F. (1973), *Proc. Natl. Acad. Sci. U.S.A. 70,* 255.
Duysens, L. N. M. (1956), *Biochim. Biophys. Acta 19,* 1.
Fenn, R. W., and Oser, H. (1965), *Appl. Opt. 4,* 1504.
Gitter-Amir, A., Schneider, A. S., and Rosenheck, K., *Biochemistry 15* (following paper in this issue).
Glaser, M., and Singer, S. J. (1971), *Biochemistry 10,* 1780.
Gordon, D. J. (1972), *Biochemistry 11,* 413.
Gordon, D. J., and Holzwarth, G. (1971), *Proc. Natl. Acad. Sci. U.S.A. 68,* 2365.
Gregory, R. P. F., and Raps, S. (1974), *Biochem. J. 142,* 193.
Gumprecht, R. O., and Sliepcevich, C. M. (1953), *J. Phys. Chem. 57,* 90.
Hanahan, D. J. (1973), *Biochim. Biophys. Acta 300,* 319.
Holzwarth, G., Gordon, D. J., McGinnes, J. E., Dorman, B. P., and Maestre, M. F. (1974), *Biochemistry 13,* 126.
Ji, T. H., and Urry, D. W. (1969), *Biochem. Biophys. Res. Commun. 34,* 404.
Latimer, P. (1972), *J. Opt. Soc. Amer. 62,* 208.
Latimer, P., and Eubanks, C. A. H. (1962), *Arch. Biochem. Biophys. 98,* 274.
Latimer, P., and Pyle, B. E. (1972), *Biophys. J. 12,* 764.
Litman, B. J. (1972), *Biochemistry 11,* 3243.
Lowry, D. H., Rosebrough, N. J., Farr, A. L., and Randall, A. J. (1951), *J. Biol. Chem. 193,* 265.
Philipson, K. D., and Sauer, K. (1973), *Biochemistry 12,* 3454.
Pilat, M. I. (1967), *Appl. Opt. 6,* 1555.
Rosenheck, K., and Schneider, A. S. (1973), *Proc. Natl. Acad. Sci. U.S.A. 70,* 3458.
Rosenkranz, H. (1974), *Z. Klin. Chem. Klin. Biochem. 12,* 415–422.
Rosenkranz, H., and Scholtan, W. (1971), *Hoppe-Seyler's Z. Physiol. Chem. 352,* 896.
Roth, S., and Seeman, P. (1972), *Biochim. Biophys. Acta 255,* 190.
Schneider, A. S. (1971), *Chem. Phys. Lett. 8,* 604.
Schneider, A. S. (1973), *Methods Enzymol. 27D,* 751.
Schneider, A. S., Schneider, M. J. T., and Rosenheck, K. (1970), *Proc. Natl. Acad. Sci. U.S.A. 66,* 793.
Schwoch, G., and Passow, H. (1973), *Mol. Cell. Biochem. 2,* 197.
Urry, D. W. (1972), *Biochim. Biophys. Acta 265,* 115.
Urry, D. W., and Ji, T. H. (1968), *Arch. Biochem. Biophys. 128,* 802.
Urry, D. W., Masotti, L., and Krivacic, J. P. (1971), *Biochim. Biophys. Acta 241,* 600.
van de Hulst, H. C. (1957), in Light Scattering by Small Particles, New York, N.Y., Wiley, p 33.
Wallach, D. F. H., Low, D. A., and Bertland, A. V. (1973), *Proc. Natl. Acad. Sci. U.S.A. 70,* 3235.